 ICCES, vol.12, no.1, pp.23-31

Numerical simulation of bi-material problems using EFGM

Ch.Raghuveer[1], Mohit Pant[1], I.V. Singh[1], B.K. Mishra[1], V. Bhasin[2]
Kamal Sharma[2], I.A. Khan[2]

Summary

In this work, element free Galerkin method (EFGM) has been applied to solve solid mechanics problems containing material discontinuities. The method is based on treatment of interface conditions at the variational level. Modifications are made in the EFGM to incorporate material discontinuities, which include the variational form of the governing differential equations. Two bi-material problems i.e. beam and bar has been solved using EFGM, and a clear discontinuity in the stress field has been observed at the interface of two materials.

Introduction

The element-free Galerkin method (EFGM) offers many advantages over standard finite element methods for the simulation of both static and dynamic solid mechanics problems. The EFGM utilizes moving least-squares interpolants which require only nodes, unencumbered by elements and elemental connectivity, to construct the shape functions. The method has mainly been applied in the area of crack propagation, where nodes were continuously moved or added to follow the crack tip. It has been found that the EFGM has higher convergence rates over the finite element method. Another advantage of the EFGM is the high-order continuity of the field variables. This allows for easy implementation of constitutive laws that include gradients of the stress or strain. However, the high-order continuity imposes a difficulty when considering material discontinuities.

In the present work, EFGM has been applied to bi-material problems. Two model problems i.e. beam and bar have been taken and analyzed by considering single domain with interface. The results obtained by EFGM are found quite satisfactory.

Review Of Element Free Galerkin Method

In EFGM, the field variable u is approximated by moving least square approximation (MLS) function $u^h(\mathbf{x})$ (Belytschko *et al.,* 1994) which is given by

$$u^h(\mathbf{x}) = \sum_{j=1}^{m} p_j(\mathbf{x}) a_j(\mathbf{x}) \equiv \mathbf{p}^T(x)\mathbf{a}(x) \tag{1}$$

where, $\mathbf{p}(\mathbf{x})$ is a vector of basis functions, $\mathbf{a}(\mathbf{x})$ are unknown coefficients, and m is the number of terms in the basis. The unknown coefficients $\mathbf{a}(\mathbf{x})$are obtained by

[1]Dept. of Mech. and Ind. Eng., IIT-Roorkee 247 667, UA, India, E-mail: iv_singh@yahoo.com, indrafme@iitr.ernet.in

[2]Reactor Structures Section, Reactor Safety Division, BARC, Mumbai, India

minimizing a weighted least square sum of the difference between local approximation, $u^h(\mathbf{x})$ and field function nodal parametersu_I. The weighted least square sum $L(\mathbf{x})$ can be written in the following quadratic form:

$$L(\mathbf{x}) = \sum_{I=1}^{n} w(\mathbf{x}-\mathbf{x}_I)[\mathbf{p}^T(\mathbf{x})\mathbf{a}(\mathbf{x}) - u_I]^2 \tag{2}$$

where, u_I is the nodal parameter associated with node I at$\mathbf{x}_I$; u_I are not the nodal values of $u^h(\mathbf{x}-\mathbf{x}_I)$ because $u^h(\mathbf{x})$ is used as an approximant and not an interpolant $w(\mathbf{x}-\mathbf{x}_I)$ is the weight function having compact support associated with node I, and n is the number of nodes with domain of influence containing the point $\mathbf{x}$, $w(\mathbf{x}-\mathbf{x}_I) \neq 0$. By setting $\partial L/\partial \mathbf{a}$=0, a following set of linear equation is obtained as:

$$\mathbf{A}(\mathbf{x})\mathbf{a}(\mathbf{x}) = \mathbf{B}(x)\mathbf{u} \tag{3}$$

By substituting Eq. (3) in Eq. (1), the approximation function is obtained as:

$$u^h(\mathbf{x}) = \sum_{I=1}^{n} \Phi_I(\mathbf{x})u_I \tag{4}$$

Governing Equations Of Bi-Material

The treatment of material discontinuity (Liu, 2003; Belytschko *et al.,* 1996) in the EFGM is demonstrated by considering a linear electrostatics. For simplicity, two distinguishable materials separated by a single interface,Γ_s as shown in **Fig. 1**. This interface is defined byn_j^-, the unit outward normal of Ω^- along the material boundary (Cordes and Moran, 1996) The governing equilibrium equation is given by

$$\sigma_{ji,j} + b_i = 0 \text{ in } \Omega \tag{5}$$

along with associated boundary conditions

$$\sigma_{ij}n_j = \bar{t}_i \text{ on } \Gamma_t \tag{6}$$

$$u_i = \bar{u}_i \text{ on } \Gamma_u \tag{7}$$

where, σ_{ij} the Cauchy stress tensor and b_i is a body force. t_i is defined as the traction on a surface, and u_i is the displacement field.

Modifications For Material Discontinuity

Few modifications are introduced in EFGM to solve bi-material problems, which gives EFGM an ability to solve problems involving material discontinuities. This method (Cordes and Moran, 1996) involves considering the inhomogeneous

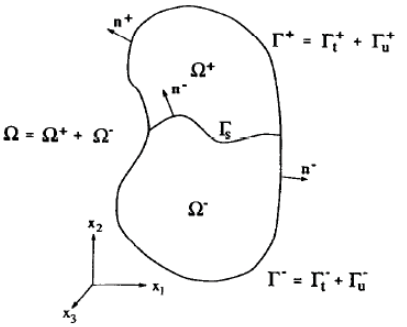

Figure 1: Three-dimensional inhomogeneous body.

medium as separate homogeneous bodies, and then applying modifications at the interface. The separation of the body into its homogeneous parts is accomplished through the weight function, specifically the domain of influence in determining the neighbors$n$. For a homogeneous part, the neighbors to a point **x** are the nodes which contain **x** in their domain of influence. The neighbors for inhomogeneous bodies are determined by defining the interface first by a set of nodes which belong to both materials. The line drawn by connecting these nodes is considered as an interface Γ_s between two materials. The domain of influence for the nodes enclosing part of the interface in either material is truncated alongΓ_s. Therefore, points contained in material-1 can only be influenced by nodes in material 1 plus interface nodes; and, points contained in material-2 can only be influenced by nodes contained in material-2 plus interface nodes.

Figs. 2 and **3** illustrate the selection of the neighbors for homogeneous and inhomogeneous materials respectively. The domains of influence are drawn only for nodes labeled 1 through 5 in each figure to determine if these labeled nodes are considered neighbors to the points ***a***, ***b*** and ***c***. The domain of influence for each node is a circle centered at the node. For the homogeneous case (**Fig. 2**), point ***a*** is contained in the domain of influence of both nodes 4 and 5; therefore, nodes 4 and 5 are considered neighbors of point ***a***. Similarly, point ***b*** has neighbors of nodes 3 and 5, and point ***c*** has neighbors of nodes 1 and 2. However, when an interface separating two materials is added as in **Fig. 3**, the neighbors to each of the points ***a***, ***b*** and ***c*** may change.

The domains of influence for node 4 and node 5 are unaffected by the inserted interface; node 4 does not intersect the interface, and node 5 is an interface node belonging to both materials. Therefore, point a still contains nodes 4 and 5 as neighbors. The domains of influence for nodes 1, 2 and 3 are each truncated at the interface. The neighbors of point b still include nodes 3 and 5 since each pertain to material 1; however, point ***c*** is not included in node 2 domain of influence due

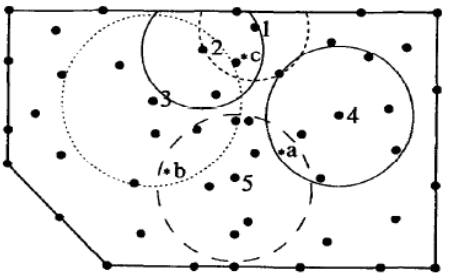

Figure 2: Domains of influence and nearest neighbors for homogeneous bodies

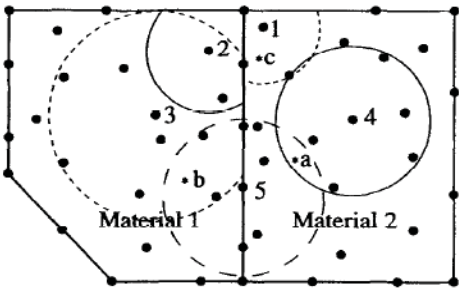

Figure 3: Domains of influence and nearest neighbors for inhomogeneous bodies

to the truncation of the domain of influence of node 2 at the interface. Point ***c*** has only one neighbor labeled in **Fig. 3**, node 1.

The following weak form of $\sigma_{ji,j}+b_i=0$ in Ω is considered in which

$$\int_\Omega \delta u_{i,j}\sigma_{ij}d\Omega-\int_\Omega \delta u_i b_i d\Omega-\int_{\Gamma_t}\delta u_i\bar{t}_i d\Gamma-\int_{\Gamma_u}\delta\lambda_i(u_i-\bar{u}_i)d\Gamma-\int_{\Gamma_u}\delta u_i\lambda_i d\Gamma=0 \tag{8}$$

the Lagrange Multipliers, λ_i, enforce the essential boundary constraint on Γ_u (Batra *et al.*, 2004) and the associated Euler Equations are

$$\sigma_{ji,j}+b_i=0 \text{ in } \Omega^+ \text{ and } \Omega^-, \tag{9}$$

$$t_i-\bar{t}_i=0 \text{ on } \Gamma_{t+} \text{ and } \Gamma_{t-}, \tag{10}$$

$$u_i-\bar{u}_i=0 \text{ on } \Gamma_{u+} \text{ and } \Gamma_{u-}, \tag{11}$$

$$\lambda_i-t_i=0 \text{ on } \Gamma_{u+} \text{ and } \Gamma_{u-}, \tag{12}$$

corresponding to the satisfaction of the equilibrium equation $\sigma_{ji,j}+b_i=0$ in Ω in both Ω^+ and Ω^-; the traction and displacement boundary conditions, $\sigma_{ji}n_j=\bar{t}_i$ on Γ_t, and $u_i=\bar{u}_i$ on Γ_u, on both Γ^+ and Γ^-; and, the physical interpretation of the Lagrange multiplier $\lambda_i=t_i$. The discretization of the above Eq. (8) after imposing boundary conditions leads to the following set of linear equations:

$$\mathbf{Ku}=\mathbf{f} \tag{13}$$

Where, the matrices ***K*** and **f** are defined as

$$K_{IJ}=\int_\Omega \mathbf{B}_I^T\mathbf{D}\mathbf{B}_J d\Omega-\int_{\Gamma_u}\phi_I\mathbf{S}\mathbf{N}\mathbf{D}\mathbf{B}_J d\Gamma-\int_{\Gamma_u}\mathbf{B}_I^T\mathbf{D}^T\mathbf{N}^T\mathbf{S}\phi_J d\Gamma \tag{14}$$

$$f_I=\int_{\Gamma_t}\phi_I\bar{\mathbf{t}}d\Gamma-\int_{\Gamma_u}\mathbf{B}_I^T\mathbf{D}^T\mathbf{N}^T\mathbf{S}\bar{\mathbf{u}}d\Gamma \tag{15}$$

$$\mathbf{D} = \frac{E}{1-\nu^2}\begin{bmatrix} 1 & \nu & 0 \\ \nu & 1 & 0 \\ 0 & 0 & \frac{1-\nu}{2} \end{bmatrix}, \quad \mathbf{B}_I = \begin{bmatrix} \phi_{I,x} & 0 \\ 0 & \phi_{I,y} \\ \phi_{I,y} & \phi_{I,x} \end{bmatrix} \tag{16}$$

$$\mathbf{N} = \begin{bmatrix} n_x & 0 & n_y \\ 0 & n_y & n_x \end{bmatrix}, \quad \mathbf{S} = \begin{bmatrix} s_x & 0 \\ 0 & s_y \end{bmatrix} \tag{17}$$

$$s_x = \begin{cases} 1, \text{ if the prescribed } u_x \text{ on } \Gamma_u \\ 0, \text{ if the prescribed } u_y \text{ on } \Gamma_u \end{cases} \tag{18}$$

$$s_y = \begin{cases} 0, \text{ if the prescribed } u_x \text{ on } \Gamma_u \\ 1, \text{ if the prescribed } u_y \text{ on } \Gamma_u \end{cases} \tag{19}$$

Results And Discussions

Case-I: Cantilever Beam

A beam of dimensions $L \times D$ is subjected to a traction at the free end as shown in **Fig. 4**. The problem has been solved for the plane stress case with material properties are taken of E_1= 2x10^{11} unit, ν_1=0.3, E_2 = 0.2x10^{11} unit, ν_2 = 0.3 and the beam dimensions are D = 1 unit, L = 4 unit. The applied traction is P = 50000 unit. The beam has been discretized using regular arrangement of nodes as shown in **Fig. 5**. In each integration cell 4×4 Gauss quadrature is used to evaluate EFGM stiffness matrix. The results are obtained using a linear basis with the cubicspline weight function and a $d_{\max}$ value of 1.2 (Krongauszs and Belytschko, 1998).

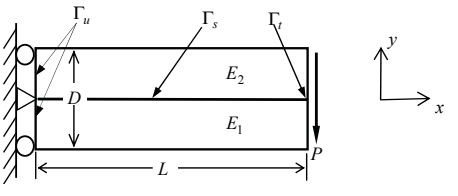

Figure 4: A two dimensional bi-material beam with traction

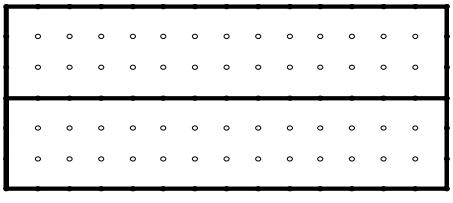

Figure 5: Regular nodes distribution for the domain of the cantilever beam

The deformed shape of beam after application of load is shown in **Fig. 6**. **Figure 7 & 8** show the distribution of the σ_{xx} and ε_{xx} over the domain respectively. From these figures, it has been observed that the stress is discontinuous at the interface of the beam i.e. at D = 0 units while strain is continuous. The distribution of σ_{xx} and ε_{xx} are shown in **Figs. 9-10** with the beam depth at centre i.e. $x = L/2$.

Case-II: Axial Bar

A bi-material bar of dimensions *LxD* is considered next, which is subjected to tensile load P at the free end as shown in **Fig. 11**. The problem has been solved for the plane stress case with material properties and dimensions same as ca*se-I*. One

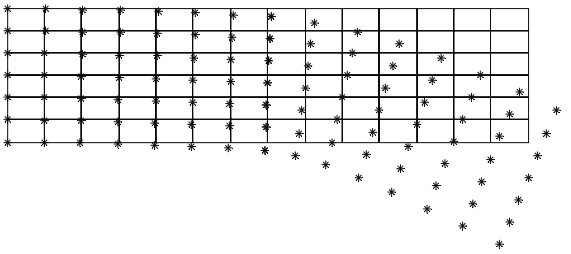

Figure 6: Displaced position of nodes after application of traction

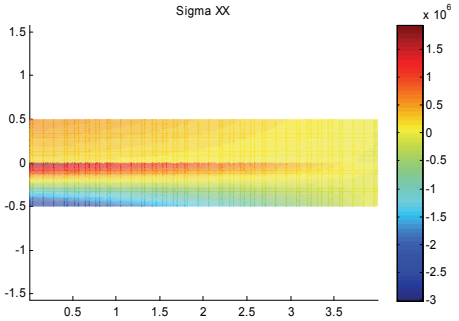

Figure 7: Distribution of σ_{xx} over the domain

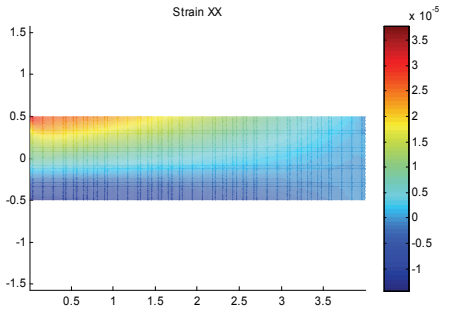

Figure 8: Distribution of ε_{xx} over the domain

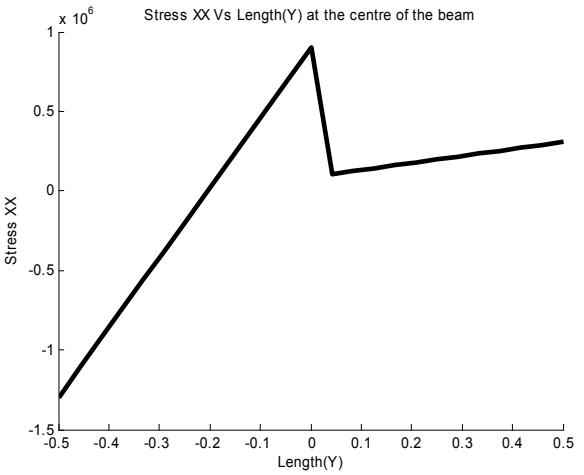

Figure 9: Distribution of σ_{xx} with depth at the centre of the beam

end of the bar is fixed while a tensile load of P = 50000 units is applied at the other end of the bar. The bar has been discretized using regular arrangement of nodes as shown in **Fig. 5**. In each integration cell 4×4 Gauss quadrature is used to evaluate stiffness the matrix. The EFGM results are obtained using a linear basis with the

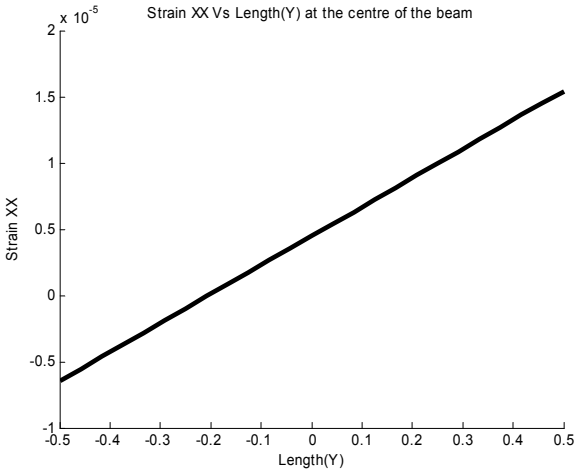

Figure 10: Distribution of ε_{xx} with depth at the centre of the beam

cubicspline weight function with $d_{\max} = 1.2$.

The deformed shape of bar after the application of load is shown in **Fig. 12**. Figures **13-14** show the distribution of the σ_{xx} and ε_{xx} over the domain respectively. The distribution of σ_{xx} and ε_{xx} with the depth of the beam are shown in **Figs. 15-16** at the center of the bar. From these figures, it can be noticed that the stress is discontinuous at the interface, while strain is continuous.

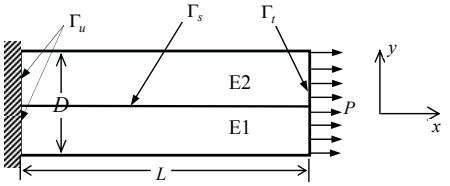

Figure 11: A two dimensional bi-material bar with tensile load

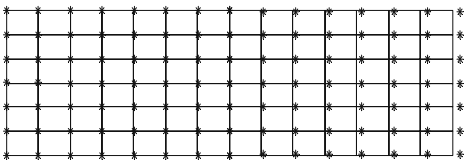

Figure 12: Displaced position of the nodes after application of tensile load

Conclusions

In this work, element free Galerkin method has been used to solve the bi-material problems. A bi-material cantilever beam with traction at the free end and a bi-material bar with uniform tensile loading at the free end of the beam are taken and solved by EFGM. Lagrange multiplier technique has been used to enforce the essential boundary conditions. Four point Gauss quadrature has been used for the numerical integration of Galerkin weak form. The stress-strain distributions are plotted over the domains of beam and bar. From the analysis it was found that the stress is discontinuous at the interface of the beam and bar, while strain is continuous. Since, EFGM is quite effective in solving the bi-material problems; therefore,

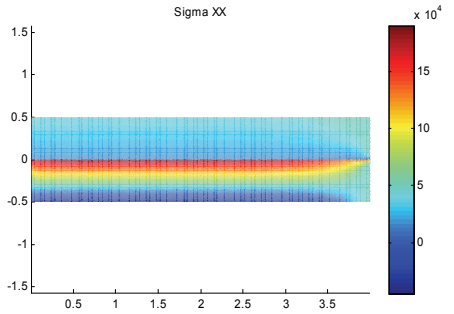

Figure 13: Distribution of σ_{xx} over the domain

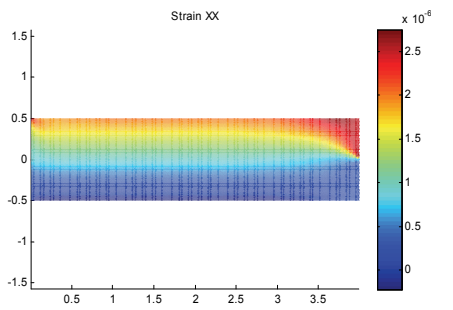

Figure 14: Distribution of ε_{xx} over the domain

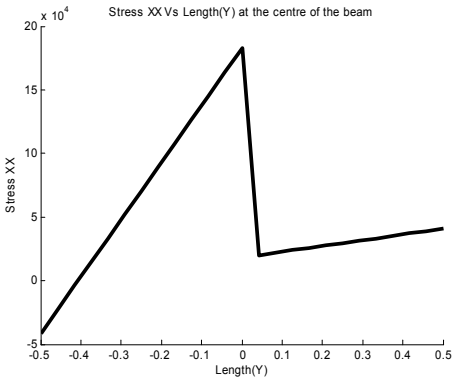

Figure 15: Variation of σ_{xx} with depth at the center of the bar

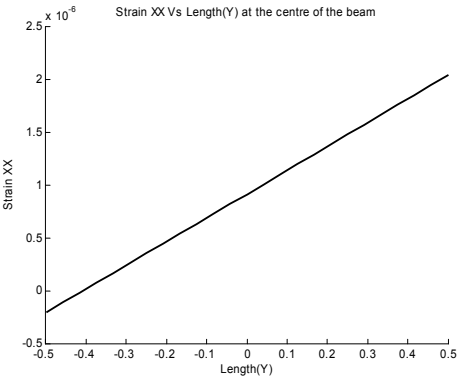

Figure 16: Variation of ε_{xx} with depth at the center of the bar

this work can be extended further to solve complex bi-material cracked components.

Acknowledgement

A part of this work is supported by Department of Atomic Energy, Bhabha Atomic Research Centre, Mumbai, Grant No.2007/36/84-BRNS/2904.

References

1. Batra, R. C., Porfiri, M. and Spinello, D., 2004 "Treatment of material discontinuity in two meshless local Petrov–Galerkin (MLPG) formulations of axisymmetric transient heat conduction", *International Journal for Numerical Methods in Engineering*, 61, pp. 2461–2479.
2. Belytschko, T. and Krongauz, Y., Organ, D., Fleming, M. and Krysl P., 1996 "Mesh-less methods: An overview and recent developments", *Computer Methods in Applied Mechanics and Engineering*, 139, pp. 3-47.
3. Belytschko, T., Lu, Y. Y. and Gu, L., 1994 "Element-free Galerkin methods",

International Journal for Numerical Methods in Engineering, 37, pp. 229-256.

4. Cordes L. W. and Moran B., 1996 "Treatment of material discontinuity in the element free Galerkin method", *Computer Methods in Applied Mechanics and Engineering,* 139, pp. 75-89.
5. Krongauz, Y. and Belytschko, T., 1998, "EFG Approximation with discontinuous derivatives" *International Journal for Numerical Methods in Engineering,* 41, pp. 1215−1233.
6. Liu, G. R., 2003, "Mesh free methods-Moving beyond the finite element method", 1st Edition, CRC Press, pp. 1-210, Boca Raton.